SUPPLEMENTARY INFORMATION

PART A: Additional Figures

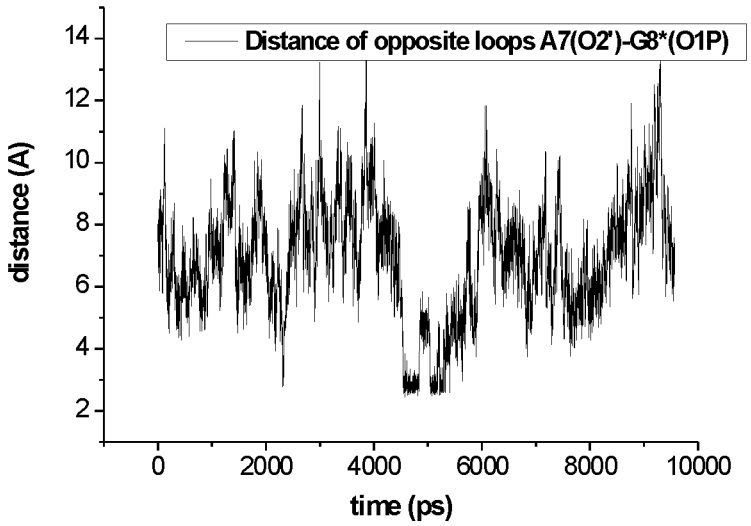

Figure S1

Figure S1.
Temporary h-bond formed during the closed state around 5 ns between opposite loops in the central part of the 2 bp kissing complex.

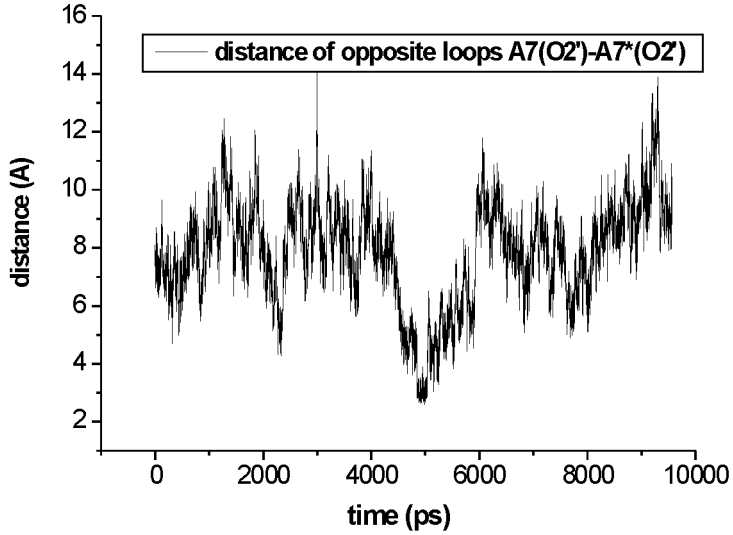

Figure S2

Figure S2.
Temporary h-bond formed during the closed state around 5 ns between opposite loops in the central part of the 2 bp kissing complex.

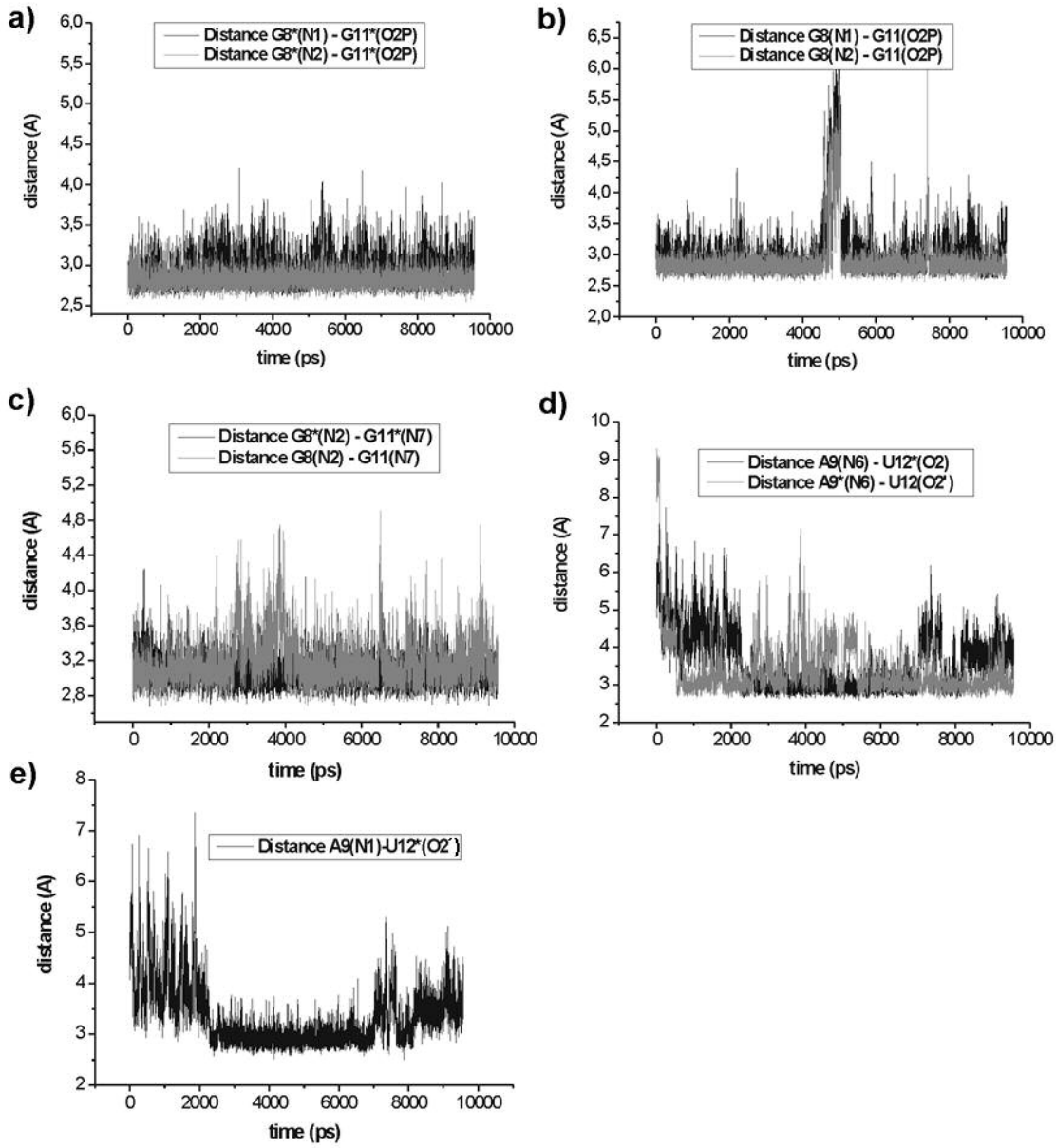

Figure S3

Figure S3.
H-bonds observed in the course of simulation kiss1 of H3 stem-loop kissing loop complex. Stable h-bond (see e) A9(N1)-U12*(O2') linking the two loops together was observed only on one side of the complex.

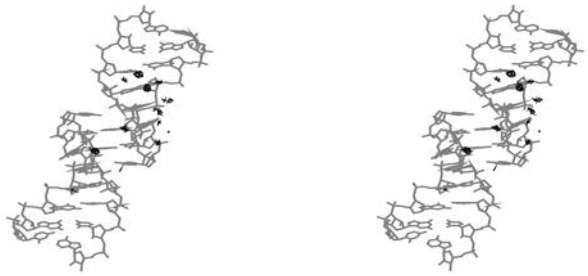

Figure S4

Figure S4.
Main hydration sites in the 2 bp kissing complex, contour level is 80.

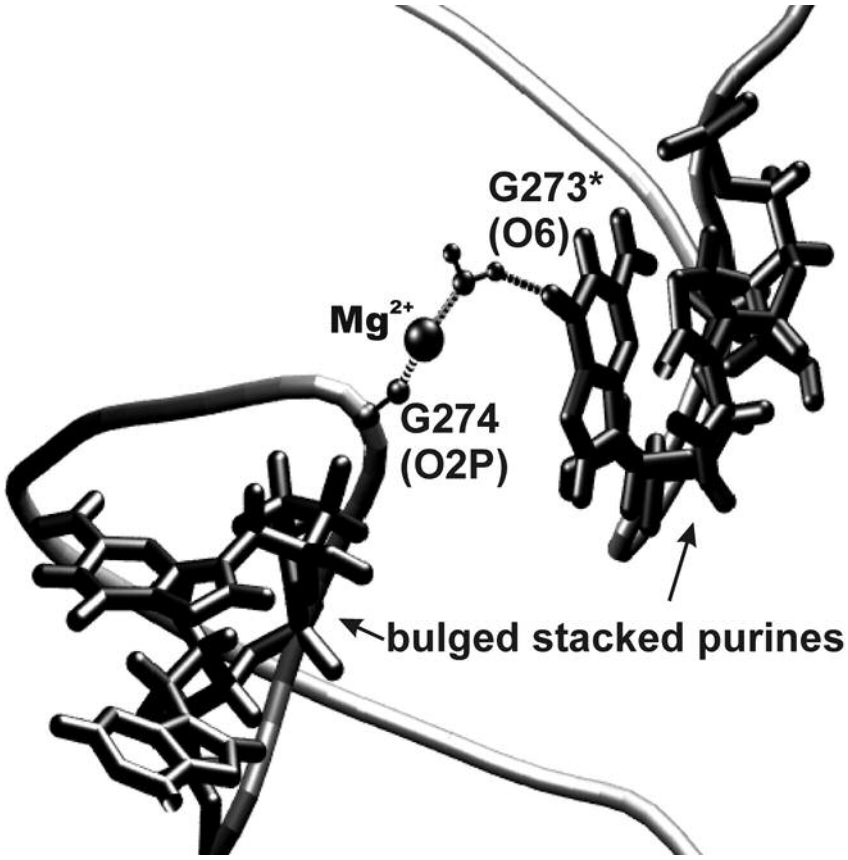

Figure S5

Figure S5.
Detail of the central pocket of the 6 bp kissing complex simulation "mal". Mg^{2+} cation is bridging the two loops via its inner shell binding to G274(O2P) and temporary water bridge to G273*(O6).

MD simulation initiated with the 6 bp kissing complex NMR structure (subtype B).

During 3 ns simulation of the NMR structure of the 6 bp kissing complex subtype B (pdb code 1BAU) the following key changes were seen.

1. The initial structure shows abundant steric clashes. The intermolecular Watson-Crick base pairs have heavy atoms in very close distances, for example: C277(N4)-G276*(O6) = 2.15 Å, C277(N3)-G276*(N1) = 1.78 Å and C277(O2)-G276*(N2) = 1.27 Å! During our MD simulation all these unacceptable close contacts improved to standard values.
2. Partial intermolecular stacking interactions seen in the NMR structure (but not seen in the X-ray structure) between A272 and A273* disappeared. The distance between A272(N7)-A273*(N7) increased from 6.6 Å (starting NMR structure) to 8 Å (after 3 ns simulation) while the A273(N7)-A272*(N7) distance increased from 6.2 Å (starting NMR structure) to 7.7 Å.
3. The NMR structure is substantially bent. The kink essentially disappeared during the MD simulation (see Figures S6, S7).
4. Bases G271 and C281 form standard WC base pair in the X-ray structure, but are not paired in the NMR structure and do not occur in one plane. They adopt in plane position after 3 ns of simulation though they do not form a base pair during the short simulation.
5. The inter-loop pocket distance is 4 Å in the starting NMR structure. After 3 ns this distance increases to 8.0 Å, i.e., close to X-ray structure (7.7 Å).

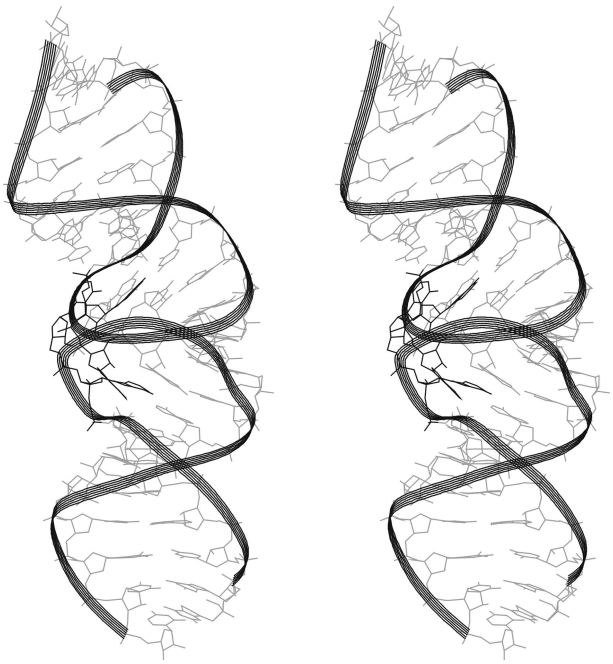

Figure S6

Figure S6.
Stereo view of the 6 bp kissing complex (subtype B) from MD simulation after 3 ns. The starting structure was taken from the NMR data. Bulged out bases A272 and A273 are shown in black.

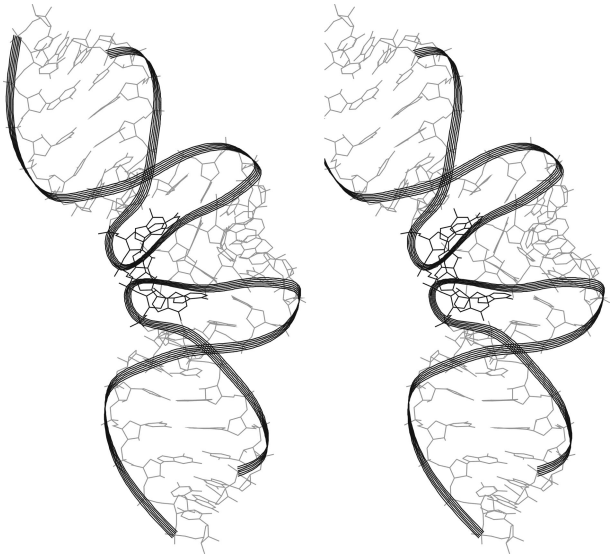

Figure S7

Figure S7.
Stereo view of the starting NMR structure of the 6 bp kissing complex (subtype B). The structure is strongly bent. Bulged out bases A272 and A273 are shown in black.

RMSd value with respect to the starting NMR structure reaches 3.2 Å after 3 ns into the simulation and appears to be further increasing.

In summary, the simulation suggests that the NMR structure is unstable and swiftly deviates essentially towards the X-ray geometry.

PART B: Additional Tables

Table S1.
Van der Waals component of stacking energy in central part of the 2 bp kissing complex during simulation kiss1. The Table shows improvement of van der Waals energy in course of the simulation except of the A9* – C13 ribose stacking that is affected by a structural asymmetry developed during the simulation (see the main text).

the first loop	VDW energy NMR structure (kcal/mol)	VDW energy 2 - 8 ns (kcal/mol)
A9 – C10	-4.4	-5.3±0.9
A9 – C13* ribose	-3.6	-3.6±0.8
A7 – G8	-5.2	-6.3±0.7
G11 – U12 ribose	-2.7	-3.5±0.8
the second loop		
A9* – C10*	-3.4	-5.2±0.7
A9* – C13 ribose	-2.9	-1.8±1.2
A7* – G8*	-5.4	-5.2±0.9
G11* – U12*	-2.6	-3.3±0.3

Table S2.
Main binding sites (inner-shell binding only) of Na^+ cations in 2 bp kissing complex (simulation "kiss1"). Note that the long-residency Na^+ cations present in the central pocket fluctuate and often are not often involved in inner-shell binding (see the text for further details).

binding sites	occupancy (%)
G8(N7)	37
A7*(N7)	24
A9(N7)	21
G8*(N7)	15
A7(N7)	14
A9*(O2P)	11
A9*(N7)	11
G6*(N7)	10
G4*(O6)	10

PART C: Quantum-chemical analysis

The NMR study reports very unusual nonplanar G=C base pairs, with a close mutual contact between the cytosine amino groups and several other unusual structural aspects. It was suggested that the kissing region is stabilized by novel electrostatic interactions as depicted in Fig. 2 (see the main text and ref. 7). However, based on our preceding extensive experience with quantum-chemical and molecular dynamics studies of nucleic acids, we were not convinced that the observed structure can be explained by such electrostatic contacts. We instead assumed that the experimental geometry could be stabilized by a substantial pyramidalization of the amino groups in the central region of the structure, accompanied by a formation of out-of-plane H-bonds and possibly also amino-acceptor interactions. Similar interactions were recently identified in nucleic acids (see the main text ref. 43). Thus, we carried out ab initio quantum chemical calculations where the intermolecular positions of key nucleobases were frozen as in the experimental structure while the monomer geometries were relaxed. Five models were considered differing in the flexibility of the amino groups: (i)

complete relaxation of all four amino groups, (ii) guanine amino groups enforced to be planar, cytosine amino groups relaxed, (iii) all amino groups planar, (iv)-(v) the same as (i) and (ii), respectively, but the amino nitrogens kept coplanar with the base. Geometry optimizations were carried out at HF level of theory with the 6-31G basis set of atomic orbitals augmented by a set of standard d-polarization functions on the amino nitrogens. Interaction energies for the optimized structures were computed at MP2 level of theory with the 6-31G*(0.25) basis set. All computations were performed with the Gaussian98 code. For more details about such calculations see main text ref. 43.

The computed results show that the major part of the energy gain achieved by the out-of-plane relaxation of the amino groups (9.8 kcal/mol) is accountable to the clash of the cytosine amino groups (8.2 kcal/mol). The highest deviation from the planarity is observed for the cytosine amino groups, where the C4-N4HH dihedral angles are 13.3° and 23.9° (see the attached Figure). The hydrogens, however, are reoriented in order to optimize the interaction within the G=C base pairs and do not establish any interaction with the adjacent base pairs. The C2-N2HH dihedral angles for the amino groups of guanines are 0.2° and 3.4° degrees. The energy gain is markedly reduced when fixing the position of the nitrogens in the plane of the nucleobases (4.6 kcal/mol in total, from which 3.6 kcal/mol is contributed by the cytosines). These observations mean that the cytosines are mutually compressed and thus major part of the energy gains is not due to formation of any inter-base attractive interaction but due to reduction of steric clashes and energy improvement of the two G=C base pairs. Pairwise interaction energies computed between all components of the tetramer have not revealed any unusual interbase interactions promoting pyramidalization of the amino nitrogens. The two G=C terms are -24.2 and -24.4 kcal/mol, respectively, while the intrastrand stacking G...C terms are -5.2 and -6.1 kcal/mol. The interstrand C...C and G...G contacts are repulsive, with interaction energies of +2.5 and +4.7 kcal/mol, respectively. Thus the overall base pair stacking would be only -4 kcal/mol, which is poor (see main text ref. 43).

In summary, the quantum chemical calculations reveal that the structure is energetically strained and do not indicate any unusual interaction between the base pairs that could stabilize the observed interbase pair geometry.

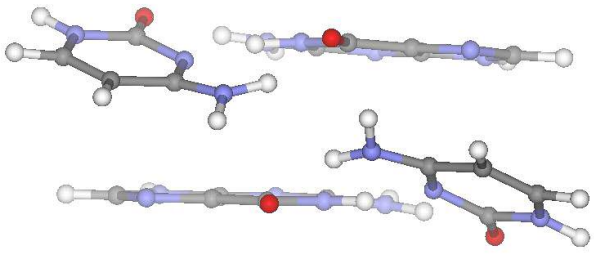

Figure: Positions of the amino groups optimised using QM calculations.

PART D: Comparison of the central part of average MD structure and refined NMR structure of the 2 bp kissing complex with the NMR restraints. Violations (bold, red) are seen for the 9 h2 – 11 h8 intramolecular and intermolecular restraints and these restraints are violated in both NMR and MD structures. Note that both violated restraints are poorly defined.

QQQQ-RRRR RRRR-QQQQ	measured NMR data	Refined NMR structure	Averaged MD structure
10 h41 – 11 o6	1.6-1.8	1.82, 1.81	1.94, 1.93
10 n3 – 11 h21	2.9-3.1	3.06, 3.11	2.70, 2.77
10 o2 – 11 h21	1.9-2.1	2.15, 2.13	1.84, 1.86
10 n3 – 11 h1	1.8-2.0	1.79, 1.82	1.94, 1.91
10 n3 – 11 n1	2.8-3.0	2.77, 278	2.92, 2.89
10 h41 – 11 h1	1.8-5	2.58, 2.64	2.27, 2.30
10 h42 – 11 h1	1.8-5	4.06, 4.12	3.84, 3.85
9 h2 – 11 h1	1.8-5	3.53, 3.23	5.13, 4.09
9 h2 – 11 h8	**3-7**	**7.11, 7.71**	**10.49, 9.06**

RRRR-RRRR QQQQ-QQQQ	measured NMR data	Refined NMR structure	Averaged MD structure
9 h1’ – 9 h2’’	1.8-3.2	2.76, 2.76	2.73, 2.69
9 h8 – 9 h1’	2.5 –5	3.82, 3.86	3.66, 3.71
9 h8 – 9 h2’’	2.5-5	3.64, 3.83	3.96, 4.01
9 h8 – 9 h3’	2.5-5	2.81, 2.58	3.12, 2.95
9 h8 – 9 h4’	3-7	4.21, 4.22	4.28, 4.28
9 h8 – 10 h5	3-7	5.25, 5.34	4.06, 4.56
9 h8 – 10 h6	3-7	5.08, 5.19	4.89, 4.95
9 h2 – 10 h1’	3-7	5.38, 5.48	3.53, 3.44
9 h2 – 11 h8	**3-7**	**7.75, 7.59**	**7.44, 7.22**
10 h1’ – 10 h2’’	1.8-3.2	2.88, 2.85	2.71, 2.76
10 h6 – 9 h1’	2.5-5	5.01, 5.04	5.06, 5.02
10 h6 – 9 h2’’	1.8-3.2	2.34, 2.35	2.46, 2.40
10 h6 – 9 h3’	2.5-5	3.68, 3.48	2.94, 3.02
10 h6 – 9 h4’	3-7	5.80, 5.92	5.53, 5.59
10 h6 – 10 h1’	2.5-5	3.50, 3.48	3.66, 3.58
10 h6 – 10 h2’’	2-4	3.91, 3.91	3.68, 3.63
10 h6 – 10 h3’	2-4	3.47, 3.65	2.51, 2.43
10 h6 – 10 h4’	3-7	4.25, 4.20	4.10, 4.16
10 h6 – 10 h5	1.8-3.2	2.44, 2.44	2.39, 2.43
10 h6 - 11 h8	3-7	4.67, 4.54	4.56, 4.61
10 h1’ – 11 h1’	3-7	6.06, 6.25	5.21, 5.19
11 h1’ – 11 h2’’	1.8-3.2	2.82, 2.83	2.68, 2.66
11 h8 – 10 h1’	2.5-5	4.96, 5.01	4.71, 4.75
11 h8 – 10 h2’’	2-4	2.34, 2.38	2.15, 2.11
11 h8 – 10 h3’	3-7	3.21, 3.14	3.27, 3.23
11 h8 – 10 h4’	3-7	5.80, 5.77	5.54, 5.58
11 h8 – 11 h1’	2.5-5	3.75, 3.76	3.75, 3.74
11 h8 – 11 h2’’	3-7	3.85, 3.94	3.95. 3.95
11 h8 – 11 h3’	3-7	3.42, 3.21	2.81, 2.95

11 h8 – 11 h4’	3-7	4.49, 4.49	4.29, 4.34

PART E: PDB files with selected averaged MD structures – separate files

2 bp kissing complex: S_kiss1.pdb, average structure 5-16 ns.

6 bp kissing complex (subtype A): S_mal.pdb, average structure 2-6.5 ns.

6 bp kissng complex (subtype B): S_lai.pdb, average structure 2-7.5 ns.